

The Magnetic Field and EUV Line Intensities in Solar Active Regions

A. Fludra¹, J. Ireland²

Abstract.

Relationships between the photospheric magnetic flux and intensities of spectral lines emitted from the solar atmosphere have been extensively studied by several authors. Power-law relations have been found between the total magnetic flux and total intensities of the chromospheric, transition region and coronal emission lines in active regions. This approach is applied to extreme ultraviolet lines recorded by the Coronal Diagnostic Spectrometer (CDS) on SOHO for 50 solar active regions, as they crossed the central meridian in years 1996-1998. Four spectral lines are examined: He I 584.3 Å (2×10^4 K), O V 629.7 Å (2.2×10^5 K), Mg IX 368.06 Å (9.5×10^5 K), and Fe XVI 360.76 Å (2.0×10^6 K). In particular, the Fe XVI 360.76 Å line, seen only in areas of enhanced heating in active regions or bright points, has not been used before for this analysis. Empirical relations are established between the total active region intensity in Fe XVI and O V lines, and the total magnetic flux and between the spatially-averaged intensities and the magnetic flux density. The dependence of the coronal loop heating rate on the magnetic flux density is derived and its implications for the coronal heating models are discussed.

1. Introduction

Our study of the relationship between the EUV line emission and the photospheric magnetic field in solar active regions is motivated by the search for the coronal heating mechanism. If well-defined relationships exist, they can be compared to theoretical predictions from the many models of coronal heating and provide constraints to identify the correct model.

Schrijver et al. (1985) and Schrijver (1987) carried out studies comparing fluxes in chromospheric and coronal EUV lines to the magnetic field. This was done for a relatively small sample of 17 active regions but was sufficient to show the presence of power-law relationships. Schrijver (1987) used Skylab data which included a chromospheric C II line, coronal Mg X 624.9 Å line and soft X-ray emission. The following relationships were found: $I_{Mg X} \propto \Phi^{1.06}$, and $I_{X-ray} \propto \Phi^{1.19}$, where I denotes the total emission line intensity summed over an active region, and Φ is the unsigned total magnetic flux. Fisher et al. (1998)

¹Rutherford Appleton Laboratory, UK

²NASA Goddard Space Flight Center, USA

confirmed the $I_{X\text{-ray}} \propto \Phi^{1.2}$ power law from a study of over 300 active regions observed by Yohkoh Soft X-ray Telescope.

The aim of this study is to find the mechanism responsible for producing these relationships. By focusing on solar active regions, one can find the dependence of the heating rate on the magnetic flux density and provide constraints on the heating mechanisms that operate in active region loops. The starting point, based on past research, is to look for power laws of the following form: $I_j \propto \Phi^{\delta_j}$, where I_j are line intensities from all layers of the solar atmosphere, and δ_j varies depending on a line: it is usually less than one for chromospheric and transition region lines, and equal to or greater than one for coronal emission.

The new, well calibrated data from the Coronal Diagnostic Spectrometer on SOHO offers an unique opportunity to study spectral lines not previously used in this type of analysis. The CDS synoptic observations include He I 584.3 Å (20,000 K), O V 629.7 Å (transition region, 2×10^5 K), Mg IX 368.06 Å (corona, 9.5×10^5 K), and Fe XVI 360.76 Å (hot corona, 2×10^6 K). The study examines 50 active regions in EUV, significantly exceeding the number studied in the only previous study of EUV/total unsigned magnetic flux correlations and power laws. The analysis uses different spectral lines than those observed by Skylab and used by Schrijver (1985, 1987). Note that whilst three of the four lines used here cover similar temperatures to those in the previous EUV study, the Fe XVI 360.76 Å line is unique - its peak emissivity is at 2 million degrees and it is a very good diagnostic of the active region temperatures. This is in contrast to the one-million degree line available in this study, which is shown to be a less useful diagnostic.

The study is also extended to derive relationships between the averaged intensities and the magnetic flux density. These results are then used to derive the dependence of the heating rate on the magnetic flux density via theoretical loop models.

2. Data Analysis and Results

For each spectral line recorded by CDS an intensity threshold is defined that separates the active region emission from the quiet sun. The area of all pixels above the threshold is measured and the total line intensity in this area is calculated.

The photospheric magnetic field is measured from the SOHO/MDI magnetograms. A threshold of 50 G is chosen to separate the active region magnetic field from the quiet sun magnetic field. An upper limit of 500 G is also used to exclude sunspots which affect the total magnetic flux of an active region but contribute only a small percentage to the coronal line emission. The total magnetic flux Φ_{tot} in the range 50 – 500 G is calculated for each active region.

2.1. Spatial Relationship Between the Coronal Emission and Photospheric Magnetic Field

Fludra et al. (1997) pointed out that active region emission at different temperatures seen in the CDS rasters is not co-spatial. In particular, hotter loops at temperatures above 1.6×10^6 K (seen in Si XII 520.7 Å and Fe XVI 360.76 Å emission) are often different from loops seen in spectral lines emitted near

1.0×10^6 K (Mg IX 360.08 Å, Mg X 624.9 Å). Since the CDS synoptic dataset contains both the Mg IX 360.08 Å line (9.5×10^5 K) and the Fe XVI 360.76 Å line (2×10^6 K), the spatial correspondence of emission in these two coronal lines can be easily compared.

Figure 1 shows that the brightest areas in the Fe XVI images are located between the opposite magnetic polarities, and the magnetic field stronger than 50 G is located close to the perimeter of the projected Fe XVI area. This spatial pattern is seen in most of the active regions. This implies that the Fe XVI emission comes from tops of coronal loops.

The Mg IX emission (9.5×10^5 K) typically exhibits a more complex behaviour: the brightest Mg IX emission is mostly located close to, or directly above the magnetic field concentrations, while the Mg IX emission between the opposite magnetic polarities is much weaker. This suggests that a significant part of the Mg IX emission comes from the legs of hot coronal loops. However, since it is known from TRACE and SOHO/EIT images that there also exist loops with peak temperatures of $1.0 - 1.2 \times 10^6$ K, part of the observed Mg IX emission must be coming from the tops of these cooler loops. Thus, the total Mg IX intensity summed over the whole active region contains a mixture of loop-top and loop-leg emission. The line intensity has a different dependence on pressure depending on the location within the loop (Martens et al. 2000): intensity of lines emitted at transition region temperatures is proportional to pressure, while the hotter loop-top emission is approximately proportional to P^2 . Thus, part of the Mg IX intensity is proportional to P and part is proportional to P^2 , making it difficult to use the total intensity summed over an active region as a diagnostic of coronal heating.

For the study of coronal heating primary interest centers on the emission coming either entirely from the loop tops or entirely from the transition region in loop legs. It is assumed that the Fe XVI emission represents loop-top emission, and hence the O V 629.8 Å line is used to the represent transition region in loop legs.

We have simulated a distribution of intensity of the Fe XVI 360.76 Å line along a static loop for loop-top temperatures between 1.6×10^6 K and 3.0×10^6 K, using a static loop model described by Martens et al. (2000) and a temperature distribution along the loop provided by P. Martens (2001, private communication). For temperatures up to 2.0×10^6 K the peak of the Fe XVI intensity is reached at the loop top. For higher temperatures, the peak intensity gradually moves away from the loop top towards the footpoints. For example, for $T_{top} = 2.5 \times 10^6$ K, the intensity peaks at 0.3 of the distance between the footpoint and the loop top, and the intensity at the top is approximately only half of the maximum intensity. This simulated behaviour of the Fe XVI intensity distribution along the loop suggests that the loops observed by CDS in the Fe XVI line cannot be significantly hotter than 2×10^6 K. If they were, the spatial distribution of intensities would show double-peaked features, with intensity peaks concentrated towards the magnetic footpoints, with lower intensities at loop tops, i.e., the pattern that is characteristic of the observed Mg IX emission (Figure 1c) but that is not seen in Fe XVI.

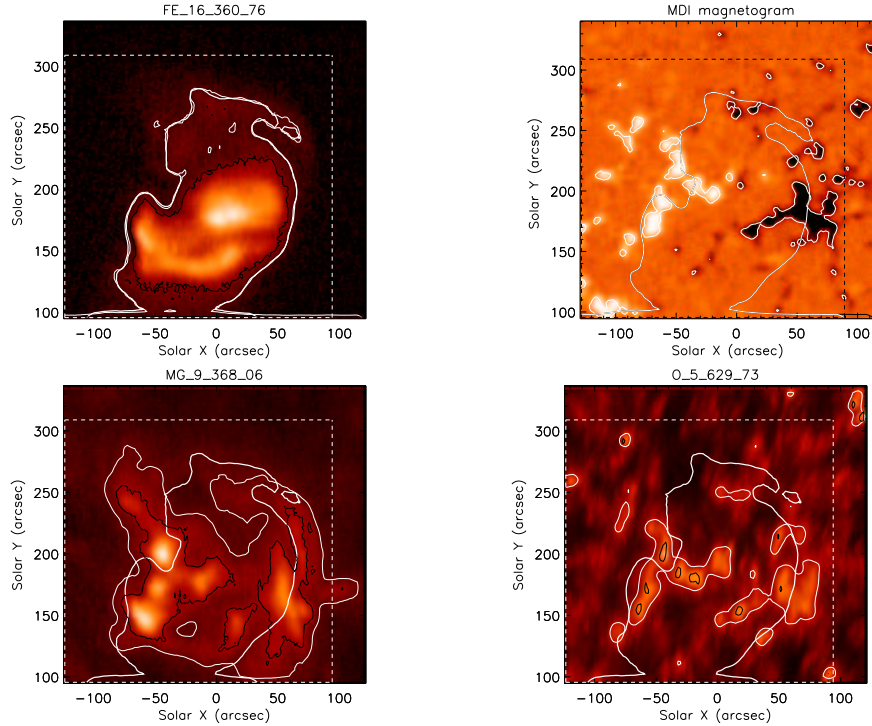


Figure 1. Comparison of the magnetic field and projected EUV emission areas in the active region NOAA 8019 on February 28, 1997: (a) Fe XVI 360.76 Å (top-left panel); (b) MDI magnetogram (top-right panel); (c) Mg IX 368.06 Å (bottom-left panel); (d) O V 629.7 Å (bottom-right panel). Thick white contour is the boundary of the Fe XVI emission. Thin white contour in the two bottom panels is the boundary of the projected area of the bright Mg IX and O V emission, respectively. Also note that the thin black contour in the bright regions encircles material twice as bright as the thin white contour.

2.2. Line Intensity–Magnetic Flux Dependence

The total unsigned magnetic flux Φ_{tot} in the range 50 – 500 G is related to the total magnetic area S_B by a power law $\Phi_{tot} = 9.21 \times S_B^{1.06}$, where the magnetic flux is expressed in [Mx] and area in cm^2 (Figure 2a). This is a nearly linear relationship with a power index of 1.06. The total magnetic flux in our sample of 50 active regions varies by a factor of 300, and the total area by a factor of 100. The magnetic flux density (i.e., total magnetic flux divided by the magnetic area) varies only by a factor of 2.3. This shows that the total magnetic flux varies primarily due to the increase in the magnetic area of the active region. This is a well established result, noticed earlier by Schrijver (1987) and Fisher et al. (1998) who comment that the increase in the total magnetic flux of active regions is mostly related to the increase of the area, and not to the increase of the field strength.

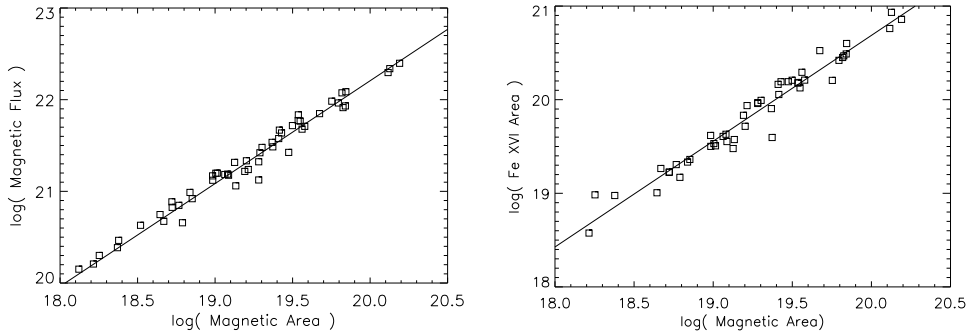


Figure 2. (a) The dependence of the total magnetic flux (Mx) on the magnetic area (cm^2) in 50 active regions (left panel); (b) The dependence of the projected Fe XVI area on the magnetic area (right panel).

Figure 2b compares the total projected area S_{Fe} of the Fe XVI emission with the total magnetic field area. As commented in Section 2.1, the Fe XVI emission originates near the loop top, while the measured photospheric B_{ph} is located at the footpoint. The projected area S_{Fe} of the emission in the Fe XVI line is related to the magnetic area S_B by the following power law: $S_{Fe} = 0.04 \times S_B^{1.13}$, where both areas are expressed in cm^2 . The power index close to 1.0 suggests that the proportion of magnetic field lines containing Fe XVI-emitting plasma is similar in all active regions, regardless of the active region size.

The total magnetic flux Φ_{tot} is found to be a good predictor of the intensity of the EUV lines. In particular, the total intensities of the two EUV lines of interest for this paper are related to the total magnetic flux by the following power laws: $I_{Fe} = 4.3 \times 10^{-5} \times \Phi^{1.27 \pm 0.05}$ for Fe XVI (Figure 3a), and $I_{OV} = 1.25 \times 10^6 \times \Phi^{0.78 \pm 0.04}$ for O V (Figure 3b). The Fe XVI power index is close to the power index of 1.2 relating X-ray luminosity and magnetic flux found by Schrijver (1987) and Fisher et al. (1998).

The correlations between the total X-ray flux and the total magnetic flux were used by Schrijver (1987) and Fisher et al. (1998) to discuss several heating models. Since the relationship between the total quantities to a large degree reflects the variation in the active region area, the total quantities are not considered to be a precise diagnostic of coronal heating. Instead, the relationships between the spatially averaged quantities are explored.

Figure 3c and d shows the relationship between the spatially averaged line intensity and the mean magnetic flux density for Fe XVI and O V. Despite a large reduction of the range of variability, these relationships for the Fe XVI and O V lines can still be approximated by a power-law. The power index for the Fe XVI $\bar{I} - \bar{B}$ dependence is 2.4, and 1.0 for O V. The error on the power index is 10% for Fe XVI and 13% for O V.

The following test was carried out: using the actual histograms of the magnetic flux density in the range 50 – 500 G in each active region, and assuming that the Fe XVI intensity of the individual loops is proportional to B_{ph}^2 , where B_{ph} is a photospheric magnetic flux density at each footpoint, the same power

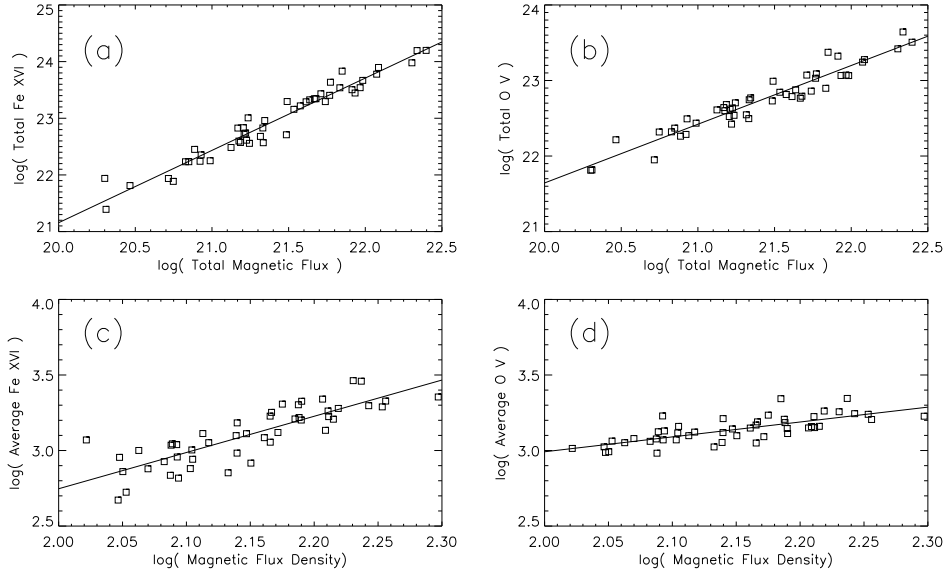


Figure 3. (a) The dependence of the total Fe XVI intensity ($\text{erg s}^{-1} \text{sr}^{-1}$) integrated over the active region area on the total magnetic flux (Mx) in 50 active regions; (b) The dependence of the total O V intensity integrated over the active region area on the total magnetic flux; (c) the dependence of the area-averaged Fe XVI intensity on the averaged magnetic flux density (Mx cm^{-2}); (d) the dependence of the area-averaged O V intensity on the averaged magnetic flux density. Magnetogram pixels with the magnetic flux density in the range 50 – 500 G were considered.

index of 2.4 in the power-law relationship between the average line intensity and the average magnetic flux density is found. On this basis one can conclude that the Fe XVI intensity in an individual coronal loop is proportional to B_{ph}^2 .

The power laws for Fe XVI and O V are used below to derive the dependence of the heating rate on the magnetic flux density.

2.3. Loop Models

Previous studies of relationships between the soft X-ray emission and the magnetic flux used the total radiative losses in soft X-rays as an approximation of the total radiative output from an active region, and compared it to the total power dissipated in the region, estimated from the Poynting flux predicted by theoretical models of coronal heating.

The energy emitted in one coronal EUV line, for example, in Fe XVI 360.76 Å, is over ten times smaller than the total energy of soft-X-rays in the range 1-300 Å (observed by Yokoh) and cannot be directly used as a measure of the total radiative loss. However, we can use loop models to deduce the line intensity dependence on the heating rate, and then derive the dependence of the heating rate on the magnetic flux density.

It is assumed that the active region loops with apex temperatures higher than 1.6×10^6 K are in a static equilibrium. This was found true for X-ray loops (Porter and Klimchuk, 1995) and the consequences of this assumption for our data are explored in this section. If the Fe XVI-emitting loops are in a static equilibrium, we can apply the scaling laws (Rosner et al. 1978; Martens et al. 2000):

$$PL = (T_{top}/C_0)^3 \quad (1)$$

$$E_H = C_1 P^{7/6} L^{-5/6} \quad (2)$$

where T_{top} , N_{top} are the electron temperature and density at the loop apex, E_H is the volumetric heating rate averaged over the whole loop, L is the loop half-length, $C_0 = 1450$, $C_1 = 1.1 \times 10^5$ in cgs units (Martens et al. 2000). The pressure $P = 2k_B N_e T_e$ is assumed constant along the loop (k_B is Boltzmann's constant).

The line intensity $I(z)$ at a distance $(z, z + dz)$ along a loop is:

$$I(z) = A_{Fe} S_{cr} N_e^2(z) G(T(z)) dz \quad (3)$$

where A_{Fe} is the iron abundance relative to hydrogen, $G(T)$ is the line emissivity and S_{cr} is loop cross-section. The electron density is expressed as $N_e(z) = P/(2k_B T_e(z))$, where pressure P relates to the apex temperature through the first scaling law (Equation 1). Thus, the total line intensity I_{tot} emitted from the whole loop is

$$I_{tot} = A_{Fe} S_{cr} / (2k_B^2) \times L \times P^2 \int_0^1 G(T(z)) / T^2(z) dz \quad (4)$$

where the integration takes place from the loop footpoint ($z=0$) to loop top (z is normalised to equal $z = 1$ at the loop top), and both halves of the loop have been added. The $G(T)$ function is calculated using ADAS software package (Summers, 1993). The temperature as a function of distance along the loop is given by Martens et al. (2000), calculated for the constant heating rate along the loop.

It is found that the dependence of the Fe XVI intensity on pressure varies depending on the peak temperature in the loop and can be approximated as $I_{tot} \propto P^a$. Values of the power index a are given in Table 1 for several temperature intervals.

These approximations are used in Section 2.4. The last row in Table 1 shows that the Fe XVI intensity is proportional to pressure for loop apex temperatures greater than 3×10^6 K. The dependence of line intensities on pressure was discussed by Martens et al. (2000) who show that for loop-top temperatures greater than 2×10^6 K, the total intensity of lines emitted in loop legs at temperatures of 10^6 K or lower (e.g., Mg IX) is proportional to pressure. Extending this argument, if $T_{top} > 3 \times 10^6$ K then the intensity of the hotter line of Fe XVI also becomes proportional to pressure. However, at these high temperatures (greater than 3×10^6 K) the Fe XVI emission would be observed predominantly in the loop legs, as discussed in Section 2.1. Since it was pointed out that most of the Fe XVI emission appears to be emitted from loop tops, it is concluded

Table 1. Power indices approximating the Fe XVI line intensity $I_{tot} \propto P^a$ and the heating rate $E_H \propto B_{ph}^\beta$ for different loop apex temperatures

Temperature interval (K)	a	β
$1.6 \times 10^6 < T_{top} < 1.9 \times 10^6$	$6 \rightarrow 2$	$7/18 \rightarrow 7/6$
$2.0 \times 10^6 < T_{top} < 2.5 \times 10^6$	2	7/6
$2.5 \times 10^6 < T_{top} < 3.0 \times 10^6$	$2 \rightarrow 1$	$7/6 \rightarrow 7/3$
$T_{top} > 3.0 \times 10^6$	1	7/3

that the condition $T_{top} > 3 \times 10^6$ K is not met in the active regions observed by CDS. Therefore, most of the Fe XVI emission arises from temperatures lower than 2.5×10^6 K. This conclusion is further supported by a measurement of an electron temperature of 2×10^6 K obtained from an extended set of spectral lines in one active region by E. Landi (2001, private communication).

The other spectral line considered in this paper, O V 629.8 Å, is emitted at sufficiently low transition region temperatures (2.2×10^5 K) and it is assumed that its intensity is always proportional to pressure.

2.4. Heating Rate Dependence on B

To derive the heating rate dependence on B_{ph} , the same temperature intervals for Fe XVI are considered as in Section 2.3 (Table 1). In each of these intervals, I_{tot} is a different function of pressure and, using the second scaling law (Equation 2), I_{tot} can be expressed in terms of the heating rate E_H . Subsequently, using the result $I_{tot} \propto B^2$ from Section 2.2, the heating rate as a function of B can be expressed as $E_H \propto B_{ph}^\beta$. Values of β derived from the Fe XVI line intensity are given in the last column of Table 1.

On the other hand, the O V intensity $I_{O V}$ in loops that reach coronal temperatures is always proportional to P , i.e., to $E_H^{6/7}$. Figure 3d shows that $I_{O V} \propto \bar{B}$, which implies $E_H \propto B^{7/6}$. This dependence on B is the same as the dependence obtained from Fe XVI in the temperature interval $2.0 - 2.5 \times 10^6$ K, and is contradictory to the case with $T_{top} > 3 \times 10^6$ K. As demonstrated earlier, these high temperatures would also require that the Fe XVI emission comes predominantly from the loop legs, while the Fe XVI images show the brightest emission coming from between the opposite polarities.

Note that although the theoretical expressions for I_{tot} and E_H contain the dependence on the loop semi-length L , the loop lengths were not measured in the CDS data and thus only the dependence of the heating rate on B_{ph} has been derived, without placing constraints on L . $E_H \propto B_{ph}^{7/6}$ is consistent with the result of Schrijver and Aschwanden (2001) obtained from simulations of solar and stellar soft X-ray emission.

To see how this result constrains the heating mechanism, the results of Mandrini et al. (2000) are used; in this work, the authors review many heating

models, characterising the heating rate as $E_H \propto B_{cor}^a L^b$, where B_{cor} is the coronal magnetic field. Among the 22 models reviewed by Mandrini et al. (2000), only two models have the heating rate proportional to B . The first one (model 4 in Table 5 of Mandrini et al. 2000) is a direct current (DC) model considering magnetic reconnection in current sheets (Parker, 1983). The second model is a model in the alternating current (AC) class, with high-frequency boundary excitation (Galsgaard and Nordlund, 1996; referred to as model 21 in Mandrini et al. 2000). These models agree best with our result. Two other models have the heating rate proportional to $B^{1.5}$ and might be considered marginally acceptable: a modification of Parker’s (1983) magnetic reconnection model done by Mandrini et al. (2000; see their model 5), and a model invoking turbulence (Einaudi et al. 1996).

3. Summary

From the analysis of 50 solar active regions observed by the Coronal Diagnostic Spectrometer on SOHO and the MDI magnetograms we have found:

- The total photospheric magnetic flux in the 50–500 G range is nearly proportional to the magnetic area.
- The total photospheric magnetic flux is a good predictor of EUV line intensities in active regions.
- Most of the 2×10^6 K emission in the Fe XVI line originates at loop tops.
- The observed spatial distributions of the Fe XVI brightness suggests that the top loop temperatures are below 2.5×10^6 K.
- A significant part of the 1.0×10^6 K emission in the Mg IX line originates in loop legs.
- A power law dependence between the total Fe XVI intensity and the total magnetic field flux ($I_{Fe} \propto \Phi^{1.27}$) is found, similar to previously described X-ray results.
- The integrated Fe XVI line intensity in a coronal loop is proportional to the footpoint magnetic flux density squared: $I_{tot} \propto B_{ph}^2$.
- The intensity of the transition region line of O V in a coronal loop is proportional to the footpoint magnetic flux density: $I_{tot} \propto B_{ph}$.
- The volumetric heating rate $E_H \propto B_{ph}^{1.17}$. This is in contrast with most DC coronal heating models which predict the heating rate proportional to B^2 .

Acknowledgments. This work was supported by the United Kingdom PPARC. SOHO is a project of international cooperation between ESA and NASA. J. Ireland acknowledges support from ESA Fellowship Programme and the European Solar Magnetometry Network. We thank Dr. P. Martens for providing a computer program to calculate loop model temperatures.

References

- Einaudi, G., Velli, M., Politano, H., and Pouquet, A. 1996, ApJ, 457, L113
 Fisher, G.H., Longcope, D.W., Metcalf, T.R., and Pevtsov, A.A. 1998, ApJ, 508, 885

- Fludra, A., Brekke, P. Harrison, R.A., Mason, H.E., Pike, C.D., Thompson, W.T., and Young, P.R. 1997, *Solar Phys.*, 175, 487
- Galsgaard, K., and Nordlund, A. 1996, *J. Geophys. Res.*, 101, 13445
- Mandrini, C.H., Demoulin, P., and Klimchuk, J.A. 2000, *ApJ*, 530, 999
- Martens, P.C.H., Kankelborg, C.C., and Berger, T.E. 2000, *ApJ*, 537, 471
- Parker, E.N. 1983, *ApJ*, 264, 642
- Porter, L.J., and Klimchuk, J.A. 1995, *ApJ*, 454, 499
- Rosner, R., Tucker, W.H., and Vaiana, G.S. 1978, *ApJ*, 220, 643
- Schrijver, C.J., Zwaan, C., Maxson, C.W., and Noyes, R.W. 1985, *A&A*, 149, 123
- Schrijver, C.J. 1987, *A&A*, 180, 241
- Schrijver, C.J., and Aschwanden, M.J. 2001, *ApJ*, (submitted)
- Summers, H.P. 1993, JET Joint Undertaking Report, JET-IR(93)06